Chinese Chemical Letters 35 (2024) 109833

Contents lists available at ScienceDirect

Chinese Chemical Letters

journal homepage: www.elsevier.com/locate/cclet

Graphene controlled solid-state growth of oxygen vacancies riched V_2O_5 catalyst to highly activate Fenton-like reaction

Mengxiang Zhu[a,1], Tao Ding[a,1], Yunzhang Li[a], Yuanjie Peng[a], Ruiping Liu[b], Quan Zou[a,b], Leilei Yang[c], Shenglei Sun[d,*], Pin Zhou[e,*], Guosheng Shi[a], Dongting Yue[a,*]

[a] Shanghai Applied Radiation Institute, State Key Lab. Advanced Special Steel, Shanghai University, Shanghai 200444, China
[b] Center for Soil Protection and land scape Design, Chinese Academy of Environmental Planning, Beijing 100041, China
[c] Zhejiang Grearth Ecological Co., Ltd., International Trade Center Office Building, Hangzhou 311400, China
[d] Institute of Balsalt Fiber in Eco-Application, School of Environmental Science and Engineering, Qingdao University, Qingdao 266071, China
[e] Research Center of secondary Resources and Environment, Changzhou Institute of Technology, Changzhou 213032, China

ARTICLE INFO

Article history:
Received 9 November 2023
Revised 26 February 2024
Accepted 25 March 2024
Available online 26 March 2024

Keywords:
Oxygen vacancies
Fenton-like
Catalysis
V_2O_5
Solid-state synthesis

ABSTRACT

Fenton-like process based on metal oxide presents one of the most hoping strategies to generate reactive oxygen species to treat refractory pollutants. The introduction of oxygen vacancies (O_Vs) can enhance the catalytic performance of metal oxides in Fenton-like reaction. In this paper, a one-step all solid-state synthesis strategy is proposed to induce oxygen defects in V_2O_5, which uses graphene to engineer the crystallization process of V-based crystals. Such approach employs graphene as a solid-catalyst to promote growth of V-based crystals owing to the ions-π interactions between graphene and VCl_3. The electron-donor O_Vs in V_2O_5@graphene can not only active H_2O_2 for the $^{\cdot}OH$ generation, but also accelerate the reduction of V^{5+} and V^{4+}, thereby ensuring defective V_2O_5@graphene/H_2O_2 system is 14.3, 28.2, and 17.3 times higher than that of graphene/H_2O_2, pure V_2O_5/H_2O_2 and graphene+V_2O_5/H_2O_2 (mechanical mixed system), respectively. Our study provides a novel synthetic strategy to design and prepare O_Vs-riched transition metal catalysts for developing advanced oxidation technologies toward higher sustainability and practicality.

Advanced oxidation processes (AOPs), with advantages of high efficiency, universality and thoroughness oxidation on organic pollutants, have become one of the promising approaches for refractory organic wastewater treatment [1–6]. As one of the most mature and diverse strategies, transition metal-based Fenton-like catalysis have been studied extensively, such reactions require no additional energy and overcome the problems of homogeneous reactions [7–11]. To achieve the highly efficient generation of reactive oxygen species, many strategies are mainly focused on tailoring transition metal-based catalysts with desired active sites generation and exposure by controlling crystal facet growth and engineering geometry structural [12–17]. These traditional strategies are always conducted in the wet conduction, which needs the solvents such as water, ethanol or ethylene glycol [18,19]. Tedious multi-step processes and harsh reaction conditions blocked the practical applications of these technologies [20–24]. Therefore, developing a facile scale-up method to create more active sites to boost transition metal-based catalysts performance still remains a major challenge.

Notably, inducing chemical defects have emerged as a promising approach for improving catalytic performance by modulating the electronic structure of transition metal-based catalysts [25–28] and solid-state synthesis method with effectively introduce defects make it easy to scale-up production [29–32]. Hence, we develop a one-step all solid-state growth strategy to precisely engineer oxygen defects in V_2O_5 that are self-assembled during the process of selective crystallization, thereby boosting the Fenton-like performance in defective V_2O_5@graphene/H_2O_2 system (0.2012 min^{-1}), which was 14.3, 28.2, and 17.3 times higher than that of graphene/H_2O_2 (0.0085 min^{-1}), pure V_2O_5/H_2O_2 (0.0043 min^{-1}) and mechanical mixed system (graphene+V_2O_5/H_2O_2 0.0070 min^{-1}), respectively. Additionally, O_Vs-riched V_2O_5@graphene exhibits an outstanding catalytic stability and degradation ability for a variety of refractory organic pollutants. Our work provides a promising synthetic strategy for transition metals in Fenton-like catalytic degradation process to produce reactive oxygen species,

* Corresponding authors.
E-mail addresses: sunshenglei@qdu.edu.cn (S. Sun), zpnhs@163.com (P. Zhou), yuedongting@shu.edu.cn (D. Yue).
[1] These authors contributed equally to this work.

https://doi.org/10.1016/j.cclet.2024.109833
1001-8417/

paving the way for sustainable water purification and material design optimization.

The graphene-controlled thermal decomposition reaction of VCl_3 to defective V_2O_5@graphene by an *in situ* one-step, all-solid-state synthesis was showed in Fig. 1a. XRD patterns indicated that as the graphene addition was below 50%, VCl_3 was mainly transformed to V_2O_5 at 400 °C for 120 min and increasing graphene can induce the further decomposition of V_2O_5 to V_2O_4 (Fig. 1b and Fig. S1 in Supporting information) [33,34]. The surface morphologies of defective V_2O_5@graphene composites were obtained by field-emission scanning electron microscopy (FESEM), which showed that V_2O_5 crystals were clearly observed on the graphene sheets (Fig. 1c). Transmission electron microscopy (TEM) and high-resolution transmission electron microscopy (HRTEM) associated with the fast Fourier transform (FFT) showed a series clear lattice fringes of 2.501 Å, 2.143 Å, 2.250 Å and 2.076 Å corresponding to the (121), (012), (131) and (022) planes of V_2O_5, thereby confirming the formation of V_2O_5 crystals on graphene surface (Figs. 1d–g, Figs. S2 and S3 in Supporting information). What is more, the magnified image in Fig. 1e clearly displayed that many dislocations and distortions (red circle) were distributed around the lattice fringes, which suggested that defective V_2O_5@graphene has a typical defect-rich structure. The X-ray photoelectron spectroscopy (XPS) analysis of V_2O_5 and V_2O_5@graphene was investigated. With the graphene regulation, the new peaks of 531.0 eV and 532.8 eV corresponding to O_Vs and -OH bonds were obtained in defective V_2O_5@graphene (Fig. S4 in Supporting information), which was absent in pure V_2O_5, thereby confirming the formation of O_Vs in V_2O_5@graphene.

Energy dispersive spectroscopy (EDS) analysis revealed that the molar ratio of V/O in defective V_2O_5@graphene, V_2O_4@graphene and pure V_2O_5 was 1:0.956, 1:1.487 and 2.128 (Table S1 in Supporting information), respectively, implying that the V atom content of defective V_2O_5@graphene was higher than that of pure V_2O_5, thereby confirming the O_Vs introduction in defective V_2O_5@graphene [35].

To better reveal the positive effect of O_Vs on Fenton-like performance, degradation experiments with Rhodamine B (RhB, 10 mg/L) as a model dye were conducted. Fig. 2a showed that RhB cannot be decoloured in the presence of only H_2O_2 or defective V_2O_5@graphene. With both defective V_2O_5@graphene and H_2O_2 addition, the degradation of RhB was extremely active and conformed to *quasi*-first-order kinetics, and the reaction rate constant (k_{obs}) was 0.1214 min^{-1}, which was much higher than that of graphene/H_2O_2 (0.0085 min^{-1}), pure V_2O_5/H_2O_2 (0.0043 min^{-1}) and mechanical mixed system (graphene+V_2O_5/H_2O_2, 0.0070 min^{-1}), respectively (Fig. 2b). The H_2O_2 dosages and solution pH values had an enormous effect on H_2O_2 activation and their influences on the RhB degradation efficiency were studied. To confirm the optimum addition of H_2O_2, the catalytic performance of V_2O_5@graphene/H_2O_2 system with different H_2O_2 addition was investigated and there was no major breakthrough in Fenton-like activity as H_2O_2 usage increasing to 200 μL (Fig. S5 in Supporting information). Thus the optimal 30 wt% H_2O_2 usage was selected as 200 μL. Notably, we found that defective V_2O_5@graphene had better catalytic activity under acidic and weak alkaline (pH range: 3–9, Fig. S6 in Supporting information). Under the optimal conditions, defective V_2O_5@graphene exhibits the highest intrinsic activity, which surpassed the most advanced heterogeneous catalysts (Fig. 2c and Table S2 in Supporting information). These findings demonstrated that graphene-controlled VCl_3 thermal decomposition can *in situ* induced O_Vs in V_2O_5@graphene, which boosts Fenton-like performance for efficient complex organic wastewater treatment.

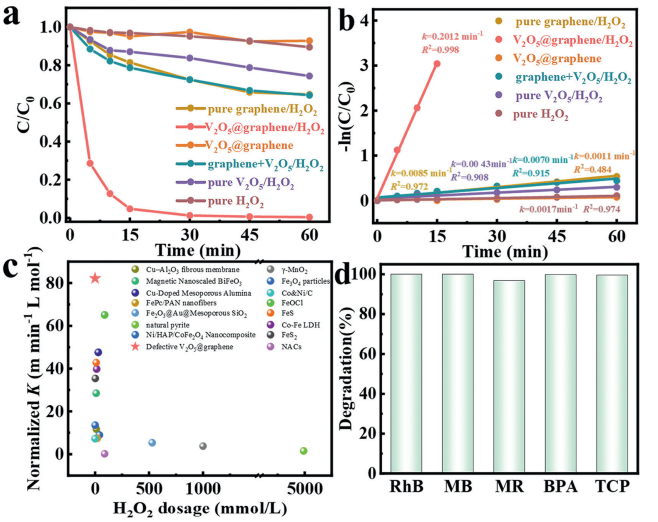

Fig. 2. (a) The degradation of RhB in pure graphene/H_2O_2, V_2O_5@graphene/H_2O_2, V_2O_5@graphene, graphene+V_2O_5/H_2O_2 and pure V_2O_5/H_2O_2 reaction systems. Reaction conditions: [catalyst] = 0.25 g/L, [H_2O_2] = 200 μL 30 wt%, [RhB] = 10 mg/L and pH 7.0. (b) Corresponding kinetic curves of the different catalytic systems. (c) Comparison of k_{obs} of different pollutant degradation *via* Fenton-like oxidation in this work and the previous reports (details in Table S2 in Supporting information). (d) Mineralization efficiency of different pollutants including RhB (10 mg/L), MB (20 mg/L), MR (20 mg/L), BPA (20 mg/L) and TCP (10 mg/L) within 4 h. Reaction conditions: [catalyst] = 0.25 g/L, [H_2O_2] = 200 μL 30 wt% and pH 7.0.

For the practical applications of defective V_2O_5@graphene/H_2O_2 system, we assessed the removal efficiency of methylene blue (MB), methyl red (MR), bisphenol A (BPA) and 2,4,6-trichlorophenol (TCP) which were universally discovered at acidic or weak alkaline environments. Fig. 2d showed that the TOC removal efficiency of RhB, MB, MR, BPA, and TCP reach up to 100%, 99.9%, 96.9%, 99.8%, and 99.6% within 6 h, confirming the excellent mineralization ability for persistent organic pollutants. In addition, catalyst stability was also tested and defective V_2O_5@graphene indicated that the defective V_2O_5@graphene/H_2O_2 system remained a high Fenton-like activity even after 12 cycles (Fig. S7 in Supporting information). During the cycle experiment, the leaching amount of V ions was investigated *via* inductively coupled plasma (ICP) and Fig. S8 (Supporting information) showed a low V ions concentration after each cycle (0.553, 0.573, 0.585 and 0.602 mg/L), confirming the stability of defects V_2O_5@graphene in Fenton-like system. Remarkably, no significant morphological changes were observed in TEM and HRTEM images (Fig. S9 in Supporting information). The XRD patterns of defective V_2O_5@graphene before and after reaction were basically identical, demonstrating that the

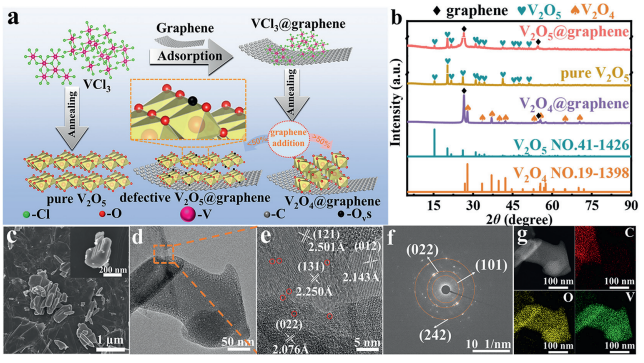

Fig. 1. (a) Schematic illustration of the sample synthesis process. (b) XRD pattern of annealed VCl_3-graphene at different mass proportions. (c) SEM and magnified SEM image of defective V_2O_5@graphene. (d,e) TEM and HRTEM image of defective V_2O_5@graphene. (f) The associated FFT analysis taken from the regions outlined in (e). (g) Elemental mapping images of defective V_2O_5@graphene.

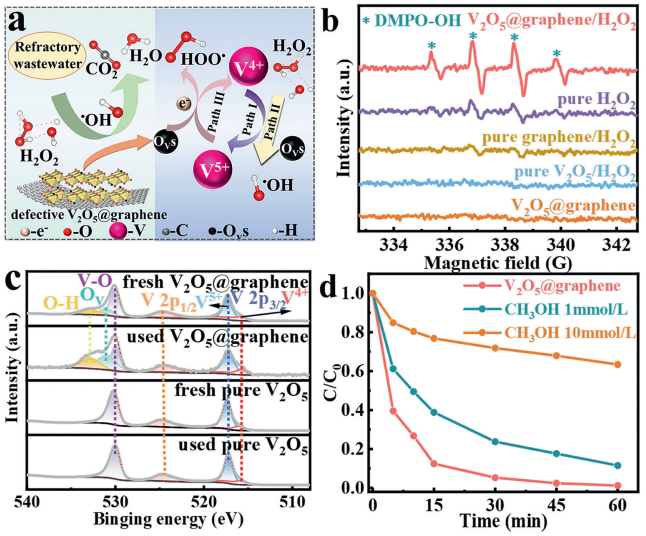

Fig. 3. (a) Schematic illustration of the Fenton-like catalysis mechanism *via* defective V_2O_5@graphene/H_2O_2 system. (b) EPR spectra of DMPO adducts in V_2O_5@graphene/H_2O_2, pure H_2O_2, pure graphene/H_2O_2, pure V_2O_5/H_2O_2 and V_2O_5@graphene reaction systems. Reaction conditions: [catalyst] = 0.25 g/L, [H_2O_2] = 200 μL 30 wt%, [DMPO] = 100 mmol/L, and pH 7.0. (c) High-resolution XPS spectrum of V 2p and O 1s of defective V_2O_5@graphene and pure V_2O_5 fresh and used. (d) The quenching experiments with existence of 1 mmol/L CH_3OH, 10 mmol/L CH_3OH in the defective V_2O_5@graphene/H_2O_2 catalytic system. Reaction conditions: [catalyst] = 0.25 g/L, [H_2O_2] = 200 μL 30 wt%, [RhB] = 10 mg/L and pH 7.0.

structure was stable (Fig. S10 in Supporting information). What is more, Fig. S11 (Supporting information) showed that the removal efficiency of BPA was achieved higher than 90.0% within 60 min even in the presence of NaCl, Na_2SO_4 and Na_2CO_3, suggesting that such defective V_2O_5@graphene/H_2O_2 system provides an effective way for saline organic wastewater treatment. These results inferred that defective V_2O_5@graphene with outstanding H_2O_2 activation and stability would be a bright Fenton-like catalyst for removing environmental organic pollutants.

On the basis of the above observations, *in situ* introduction of O_Vs in defective V_2O_5@graphene plays an important role for Fenton-like performance and the enhanced mechanism of defective V_2O_5@graphene was proposed as shown in Fig. 3a. Besides the redox cycle of V^{4+}/V^{5+} in defective V_2O_5@graphene for H_2O_2 activation, the O_Vs of electron-donor nature can not only active H_2O_2 for the $^{\bullet}OH$ generation, but also facilitate the reduction of V^{5+} to V^{4+}, thereby boosting the Fenton-like performance in defective V_2O_5@graphene/H_2O_2 system (Fig. 3a). This result was consistent with the previous research that the primary process of generating $^{\bullet}OH$ was the single electron transfer from surface V^{4+} to H_2O_2 (Eq. 1), and a chain reaction can be propagated as V^{4+} can be regenerated *via* H_2O_2 (Eq. 2) [36].

$$V^{4+} + H_2O_2 \rightarrow V^{5+} + {}^{\bullet}OH + OH^- \quad (1)$$

$$V^{5+} + H_2O_2 \rightarrow V^{4+} + HOO^{\bullet} + H^+ \quad (2)$$

The presence of O_Vs can maintain the electrostatic equilibrium, which facilitates the absorption of a large number of oxygen species, thereby promoting catalytic oxidation reactions and radical reactions [37]. Additionally, towards the oxides with surface O_Vs, interaction mode between O_Vs and H_2O_2 was a novel but overlooked reaction way for the H_2O_2 activation (Eq. 3) [38].

$$O_Vs + H_2O_2 \rightarrow {}^{\bullet}OH + OH^- \quad (3)$$

The electron paramagnetic resonance (EPR) analysis showed that DMPO−OH (1:2:2:1) signals produced in defective V_2O_5@graphene/H_2O_2 system was much higher than that in systems of pure H_2O_2, V_2O_5/H_2O_2 and graphene+V_2O_5/H_2O_2, which demonstrated the positive effect for H_2O_2 activation with the help of O_Vs (Fig. 3b).

To better insight into this mechanism, we used XPS analysis to analyze chemical state of catalysts before and after reaction (Fig. 3c). Two peaks located at 517.3 eV and 515.8 eV in the V $2p_{3/2}$ XPS spectra of pristine V_2O_5 and V_2O_5@graphene were assigned to the V^{5+} and V^{4+} signals, respectively. After Fenton-like reaction, the peak intensity of surface -OH groups (532.8 eV) were improved significantly, which was attributed to the H_2O_2 activation by O_Vs in V_2O_5@graphene [38,39]. Interestingly, the molar ratio of V^{5+}/V^{4+} in V_2O_5@graphene before and after reaction was 1.27:1 and 1.80:1, while the increase amount of V^{5+} was much lower than that of pure V_2O_5 before and after reaction (3.51:1 and 5.71:1), suggesting that the electron-rich O_Vs can suppress high value vanadium (V^{5+}) formation. Therefore, defective V_2O_5@graphene with rich O_Vs ensures the high efficiency and stable for Fenton-like catalysis. In addition, to determine the source of the electrons, we fabricated the V_2O_5@graphite, V_2O_5@CNT, and V_2O_5@graphene through the solid phase synthesis method. Interestingly, the catalytic performance of V_2O_5@graphene was much higher than that of V_2O_5@graphite and V_2O_5@CNT (Fig. S12 in Supporting information), which demonstrated that the formed electron-rich O_Vs gives electron to accelerate the high value vanadium (V^{5+}) reduction. The H_2O_2 activation performance of defective V_2O_5@graphene and pure V_2O_5 was independent of the BET surface areas of the catalysts (Table S3 and Figs. S13a-d in Supporting information), indicating that the binding capacity of the catalysts with H_2O_2 was mainly related to their chemical structure. The radical quenching experiments were further conducted to explored the roles of the reactive species in pollutant degradation. The different concentrations of methanol ($^{\bullet}OH$ scavengers [40,41]) addition significantly inhibited the RhB degradation, which suggested that the $^{\bullet}OH$-radical pathways dominated the RhB degradation in the V_2O_5/H_2O_2 catalytic system (Fig. 3d).

In summary, the vacancy defective V_2O_5@graphene with rich O_Vs was successfully prepared by solid phase synthesis method. Defective V_2O_5@graphene provides sufficient O_Vs, which can not only active H_2O_2 for the $^{\bullet}OH$ generation, but also accelerate the electron transfer from V^{5+} to V^{4+}, which make defective V_2O_5@graphene a bright Fenton-like catalyst for removing environmental organic pollutants. The defective V_2O_5@graphene/H_2O_2 system presents outstanding activity and stability for $^{\bullet}OH$ generation, which can degrade organic pollutants efficiently.

Declaration of competing interest

The authors declare that they have no known competing financial interests or personal relationships that could have appeared to influence the work reported in this paper.

Acknowledgments

This work was supported by the National Key R&D Program of China (No. 2019YFC1803900), the National Natural Science Foundation of China (Nos. U1932123, 22073069, 21773082, and 42107402), the National Science Fund for Outstanding Young Scholars (No. 11722548), and the University of Chinese Academy of Sciences (No. WIUCASOD2021014).

Supplementary materials

Supplementary material associated with this article can be found, in the online version, at doi:10.1016/j.cclet.2024.109833.

References

[1] F. Yang, B. Sheng, Z. Wang, et al., J. Hazard. Mater. 406 (2021) 124774.
[2] V. Sarria, M. Deront, P. Péringer, C. Pulgarin, Appl. Catal. B: Environ. 40 (2003) 231–246.
[3] J.L. Wang, L.J. Xu, Cri. Rev. Environ. Sci. Technol. 42 (2012) 251–325.
[4] Z.H. Xie, C.S. He, D.N. Pei, et al., Chem. Eng. J. 468 (2023) 143778.
[5] S. Feijoo, X. Yu, M. Kamali, L. Appels, R. Dewil, Rev. Environ. Sci. Biotechnol. 22 (2023) 205–248.
[6] H. Weng, Y. Yang, C. Zhang, et al., Chem. Eng. J. 453 (2023) 139812.
[7] L. Gu, N. Zhu, L. Wang, X. Bing, X. Chen, J. Hazard. Mater. 198 (2011) 232–240.
[8] M. Gągol, A. Przyjazny, G. Boczkaj, Chem. Eng. J. 338 (2018) 599–627.
[9] F. Mo, C. Song, Q. Zhou, et al., Proc. Natl. Acad. Sci. U. S. A. 120 (2023) e2300281120.
[10] Y. Li, J. Xu, G. Shi, D. Yue, Chem. Commun. 59 (2023) 1341–1344.
[11] D. Yue, X. Yan, C. Guo, X. Qian, Y. Zhao, J. Phys. Chem. Lett. 11 (2020) 968–973.
[12] Y. Xue, Q. Sui, M.L. Brusseau, et al., Chem. Eng. J. 353 (2018) 657–665.
[13] P. Salgado, V. Melin, M. Albornoz, H, et al., Appl. Catal. B: Environ. 226 (2018) 93–102.
[14] Q. Yi, J. Ji, B. Shen, et al., Environ. Sci. Technol. 53 (2019) 9725–9733.
[15] D. Yue, C. Guo, X. Yan, et al., Chem. Eng. J. 360 (2019) 97–103.
[16] D.Q. He, Y.J. Zhang, D.N. Pei, et al., J. Hazard. Mater. 382 (2020) 121090.
[17] Q. Ji, L. Bi, J. Zhang, H. Cao, X.S. Zhao, Energy Environ. Sci. 13 (2020) 1408–1428.
[18] C. Li, X. Han, F. Cheng, et al., Nat. Commun. 6 (2015) 7345.
[19] P. Zhang, L. Wang, S. Yang, et al., Nat. Commun. 8 (2017) 15020.
[20] S.W.K. Andreas Stein, T.E. Mallouk, Science 259 (1993) 1558–1564.
[21] M. Bianchini, J. Wang, R.J. Clement, et al., Nat. Mater. 19 (2020) 1088–1095.
[22] J. Diao, Y. Qiu, S. Liu, et al., Adv. Mater. 32 (2020) e1905679.
[23] R. Li, D. Speed, D. Siriwardena, et al., Chem. Eng. J. 425 (2021) 131785.
[24] K. Paździor, L. Bilińska, S. Ledakowicz, Chem. Engin. J. 376 (2019) 120597.
[25] J.J. Ye, P.H. Li, H.R. Zhang, et al., Adv. Funct. Mater. 33 (2023) 2305659.
[26] J. Chen, X.Y. Chen, Y. Liu, et al., Energ. Environ. Sci. 16 (2023) 792–829.
[27] Y. Wen, J. Yan, B. Yang, Z. Zhuang, Y. Yu, J. Mater. Chem. A 10 (2022) 19184–19210.
[28] W. Shao, M. Xiao, C. Yang, et al., Small 18 (2022) e2105763.
[29] J.R. Chamorro, T.M. McQueen, Acc. Chem. Res. 51 (2018) 2918–2925.
[30] S.R. Bauers, S.R. Wood, K.M. Jensen, et al., J. Am. Chem. Soc. 137 (2015) 9652–9658.
[31] S. Ahlawat, K.R. Mote, N.A. Lakomek, V. Agarwal, Chem. Rev. 122 (2022) 9643–9737.
[32] O. Bubnova, C. Pastore, W. Sun, A. Weingarten, ACS Nano 13 (2017) 12772–12779.
[33] T. Chirayil, P.Y. Zavalij, M.S. Whittingham, Chem. Mater. 10 (1998) 2629–2640.
[34] N. Bahlawane, D. Lenoble, Chem. Vap. Deposition 20 (2014) 299–311.
[35] Y. He, C. Chen, Y. Liu, et al., Nano Lett. 22 (2022) 4970–4978.
[36] G. Fang, Y. Deng, M. Huang, et al., Environ. Sci. Technol. 52 (2018) 2178–2185.
[37] X. Liu, J. Wu, S. Zhang, et al., Appl. Catal. B: Environ. 320 (2023) 121994.
[38] H. Li, J. Shang, Z. Yang, et al., Environ. Sci. Technol. 51 (2017) 5685–5694.
[39] L. Zhang, S. Wang, C. Lu, Anal. Chem. 87 (2015) 7313–7320.
[40] Y. Yang, G. Banerjee, G.W. Brudvig, J.H. Kim, J.J. Pignatello, Environ. Sci. Technol. 52 (2018) 5911–5919.
[41] X. Li, X. Liu, C. Lin, et al., Chem. Eng. J. 382 (2020) 123013.